07.3

Contribution of additional waveguides to heterostructure resistance of high-power coupled-waveguide-based InGaAs/GaAs/AlGaAs edge-emitting lasers

© A.S. Payusov[1], G.O. Kornyshov[1,2], N.Yu. Gordeev[1], A.E. Zhukov[3]

[1] Ioffe Institute, St. Petersburg, Russia
[2] Alferov Federal State Budgetary Institution of Higher Education and Science Saint Petersburg National Research Academic University of the Russian Academy of Sciences, St. Petersburg, Russia
[3] National Research University Higher School of Economics, St. Petersburg, Russia
E-mail: plusov@mail.ioffe.ru

Received September 20, 2023
Revised October 20, 2023
Accepted October 22, 2023

The results of numerical simulation of band diagrams and current-voltage curves of edge-emitting lasers are presented, where two additional waveguides located on the *n*-side of the heterostructure are used to suppress parasitic optical modes of the broadened waveguide. It is shown that the considered design allows obtaining the ultimate shift of the active region towards the *p*-emitter while preserving the fundamental mode lasing. The contribution of additional waveguides to the specific series resistance of the laser heterostructure estimated to be as low as $1.9 \cdot 10^{-6}\,\Omega \cdot \mathrm{cm}^2$, which does not exceed 5% of the total series resistance of up-to-date high-power InGaAs/GaAs/AlGaAs lasers.

Keywords: semiconductor laser, optical waveguide, series electrical resistance.

DOI: 10.61011/0000000000

In recent years significant progress has been made in increasing the electrical-to-optical power conversion efficiency (PCE) of semiconductor InGaAs/GaAs/AlGaAs broad area edge-emitting lasers [1] due to the design improvements of laser heterostructures. In order to achieve high PCE, it is essential to ensure low internal optical loss (α_i) and minimize the voltage drop across the laser. The voltage drop across the $p-n$-junction remains unchanged at pumping well above the threshold current, and the voltage growth with current is determined by the series resistance of the laser (R_s), which includes the resistances of the contacts and heterostructure materials as well as the resistance of the heterojunctions. The latter can comprise as much as 75% of the total resistance of the heterostructure [2].

One of the approaches which ensures laser operation on the fundamental vertical mode of a broadened waveguide with low internal optical losses is resonant suppression of parasitic modes due to additional waveguides in the CLOC (coupled large optical cavity) structure [3]. Since the fundamental mode is localized in the main waveguide stronger than others, small changes in refractive indices during laser operation at high pumping levels do not deteriorate the far-field pattern. Additional waveguides are doped in order to increase the intrinsic optical loss for parasitic modes as well as to reduce series resistance. CLOC lasers with one additional waveguide on the *n*-side and the active region shifted towards the *p* emitter (the distance from the waveguide–emitter hetero-interface is about $0.3\,\mu$ m) demonstrated low optical losses, low electrical and thermal resistances, which allowed to increase the PCE up to 57% and obtain over 12 W optical power in continuous wave (CW) operation limited by catastrophic optical degradation of laser mirrors [4]. An appropriate number of additional waveguides are used in order to suppress several parasitic modes in the CLOC structure [5]. However, unwanted voltage drop may occur at the heterojunctions of the layers forming additional waveguides of the CLOC heterostructure. Preliminary quantitative evaluations are necessary for reliable experimental verification of the contribution of additional waveguides to R_s. The aim of the present work was to investigate the effect of additional waveguides on the series resistance of heterostructure of high-power CLOC lasers using numerical simulation.

The numerical computations were performed in the SiLENSe software tool included in the SimuLED Laser Edition simulation package (STR/Soft Impact) [6]. An InGaAs/GaAs/AlGaAs heterostructure with two additional waveguides tuned to suppress the first and second optical modes of the main waveguide (CLOC 1+2, Fig. 1, *a*) was designed for the calculations. The two additional GaAs waveguides are located on the *n*-side of the heterostructure. The thickness of the main GaAs waveguide is $1.55\,\mu$m, the additional waveguides — 0.6 and $0.28\,\mu$m. The cladding layers and the $0.25\,\mu$m interlayer between the waveguides are made of $Al_{0.25}Ga_{0.75}As$ with a doping level of$2 \cdot 10^{18}\,\mathrm{cm}^{-3}$, additional waveguides have the same doping level. The experimentally obtained mobility values for electrons of 2000 and $600\,\mathrm{cm}^2/(\mathrm{Vs})(\mathrm{cm}^2 \cdot \mathrm{s})$ in GaAs and $Al_{0.25}Ga_{0.75}As$, respectively, were used. The thickness of *n*-cladding is $1.5\,\mu$m, *p*-cladding — $0.5\,\mu$m. *p*-GaAs contact

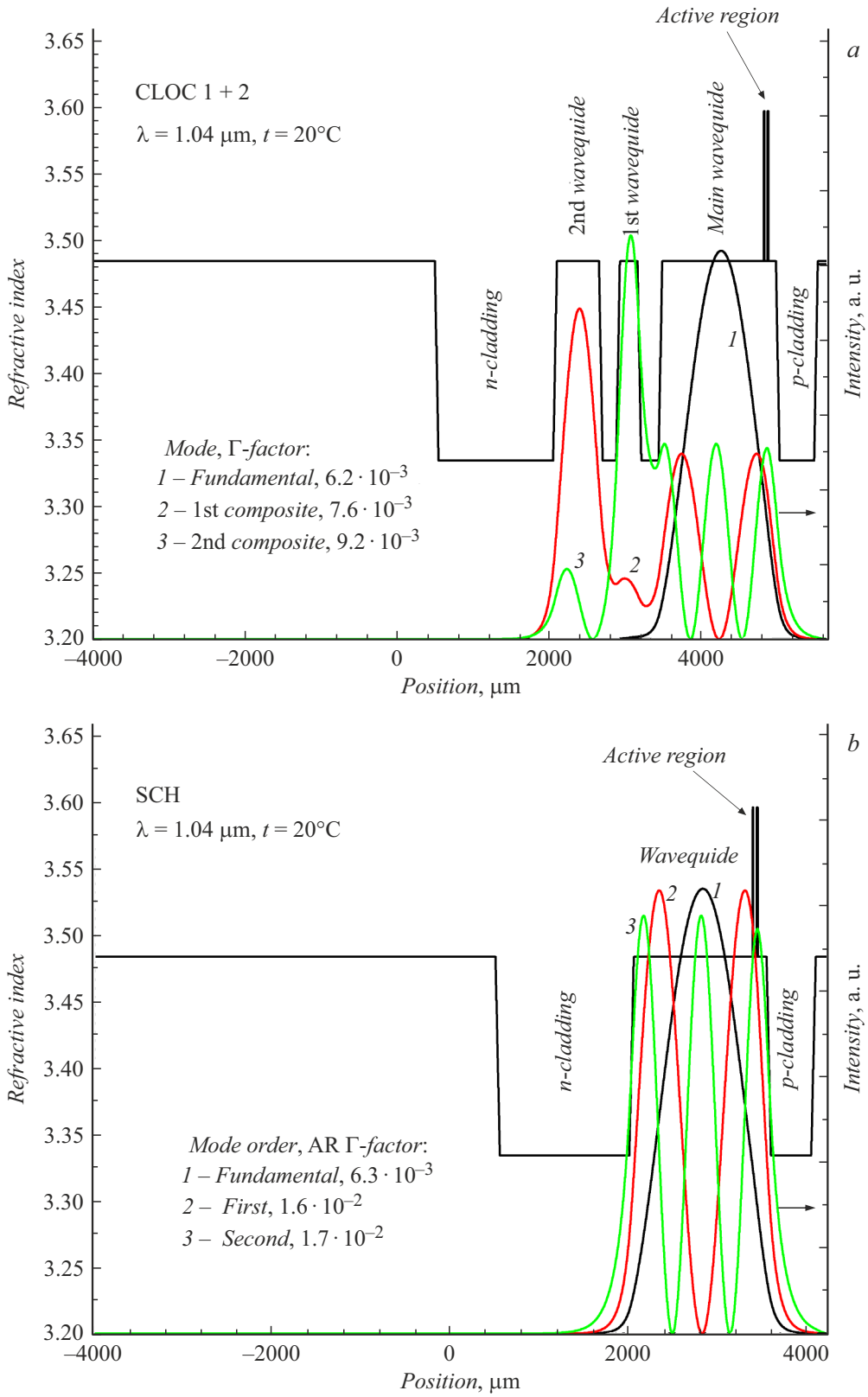

Figure 1. Refractive index profile and intensity distribution of optical modes for CLOC (*a*) and SCH (*b*) structures. The Γ-factors for waveguide modes are shown in legend.

layer 0.15 μm thick, doped to 10^{19} cm^{-3}. The doping doping level of the 150 nm thick layers adjacent to the waveguide is reduced to $5 \cdot 10^{17}$ cm^{-3} in order to reduce the losses for the fundamental mode due to free carrier absorption. The active region consists of two InGaAs quantum wells separated by 40 nm GaAs and is shifted towards the *p*-emitter as much as possible. The energy of the ground state transition of both quantum wells correspond to wavelength $\lambda = 1.04\,\mu$m. The lying depth of the active region from the surface of the structure is 0.75 μm. The graded-index GaAs$-$Al$_{0.25}$Ga$_{0.75}$As layers with a thickness of 50 nm are used to reduce the series resistance of the heterojunctions. Linear gradients of dopants concentrations were set at the boundaries of the doped layers to bring the numerical simulations closer to real heterostructrures. For the *n*-type dopant, the thickness of the gradient layer was 50 nm, and for the *p*-type dopant — 100 nm. In the reference structure, which is a laser with a rectangular waveguide (separate confinement heterostructure (SCH) (Fig. 1, *b*), and in all other parameters it is similar to the CLOC 1+2 structure.

Due to the strong shift of the active region, the optical confinement factor (Γ-factor) for the fundamental mode in the CLOC 1+2 structure is slightly lower (0.62%) than that for the composite modes (0.76 and 0.92%) (Fig. 1, *a*). In this case, stable operation on the fundamental vertical mode is ensured due to high internal optical losses for the first and second composite modes. Using the absorption cross section data and the calculated optical mode profiles, we have estimated the internal losses due to free carrier absorption [7]. They were 0.25, 4.6, and 4.7 cm^{-1} for the fundamental, first, and second composite modes, respectively.

In reference structure, the Γ-factor for the fundamental mode has almost the same value (0.63%) as in CLOC 1+2, since the intensity profile of the fundamental mode is practically unaffected by additional waveguides. Γ-factors in the SCH structure for parasitic modes appear to be about 2 times larger than in CLOC 1+2 (Fig. 1, *b*). This will result in the lasing of SCH laser on either the first or second composite mode at the beginning. However, only the fundamental mode was considered in our simulations in both lasers. These data emphasize the effectiveness of using additional optically coupled waveguides to suppress the high-order mode lasing.

While simulating the current-voltage (CV) characteristics, the width of the stripe contact was assumed to be 100 μm, and the cavity length — 4 mm. The series resistances of the substrate and metal contacts were not taken into account as they contribute equally in all structures. The temperature for all calculations was 20°C. The threshold current density was 390 A/cm^2, the laser generation wavelength — 1.04 μm provided that both lasers were operated in the fundamental mode.

The energy band diagrams of lasers at direct bias are of most interest. Comparing them for the CLOC 1+2 and SCH structures (Fig. 2, *a* and *b* respectively), one can see that the additional waveguides form a shallow potential well for electrons (insets in Fig. 2, *a* and *b*). The height of the potential barrier at the *n*-emitter interface of the waveguide is the same in both structures. Due to the reduced doping degree in the *n*-emitter near the waveguide, the potential barrier for electrons at the waveguide entrance has a step-like shape.

Increasing the thickness of the structure and introducing two potential barriers for electrons with a height of about 15 meV lead to a higher voltage drop on the CLOC 1+2 heterostructure than on the reference one at the same current density (Fig. 3). The specific series resistance of the additional waveguides can be determined from the slope of the dependence of the voltage drop difference vs current density, it was amounted to$1.9 \cdot 10^{-6}\,\Omega \cdot$ cm^2. The specific series resistance of the whole SCH heterostructure determined on the linear section of the simulated CV characteristic was found to be$1.2 \cdot 10^{-5}\,\Omega \cdot$ cm^2. In a real laser, the series resistance of the substrate, metal contacts, and laser heatsink is added to the resistance of the heterostructure itself, so that the total specific series resistance is typically makes up to $(5-9) \cdot 10^{-5}\,\Omega \cdot$ cm^2. Comparing the obtained ρ_s value of additional waveguides with the experimentally measured ρ_s values of lasers with different waveguide designs (see table), one can see that their contribution does not exceed 5%. It is possible to reduce the ρ_s of the laser by an order of magnitude $10^{-5}\,\Omega \cdot$ cm^2 by improving crystalline quality and optimizing doping profiles and composition of gradient layers [8]. The specific series resistance of metallic contacts is of the same order, according to the [9].

Thus, the series resistance of a CLOC-laser heterostructure with two additional waveguides located on the *n*-side marginally differs from that of modern high-power lasers with asymmetric heterostructure designs. Reducing the resistance of the metal contacts and optimization of the doping profiles of the heterostructure can reduce the series resistance by a much greater value than that of the additional waveguides. The inherent deviation in mentioned parameters during the fabrication and mounting process of lasers will lead to a dispersion of the series resistance of devices and will make experimental study of the resistance difference between CLOC and SCH heterostructures difficult. We also note that the use of more than two additional waveguides in high-power CLOC lasers is unnecessarily complicated, since one can already extend the main waveguide to 4.8 μm using the CLOC 1+2 design [5], and there is no need to suppress more than two optical modes in a moderately thick waveguide.

In conclusion, for the first time a numerical study of the contribution of additional waveguides to the series resistance of a CLOC InGaAs/GaAs/AlGaAs heterostructure with two additional waveguides and the maximum possible shift of the active region to the *p*-contact has been carried out. It was shown that the increase of specific series resistance by $1.9 \cdot 10^{-6}\,\Omega \cdot$ cm^2 due to the increase of heterostructure thickness and forming additional potential barriers at heterojunctions is an order of magnitude smaller

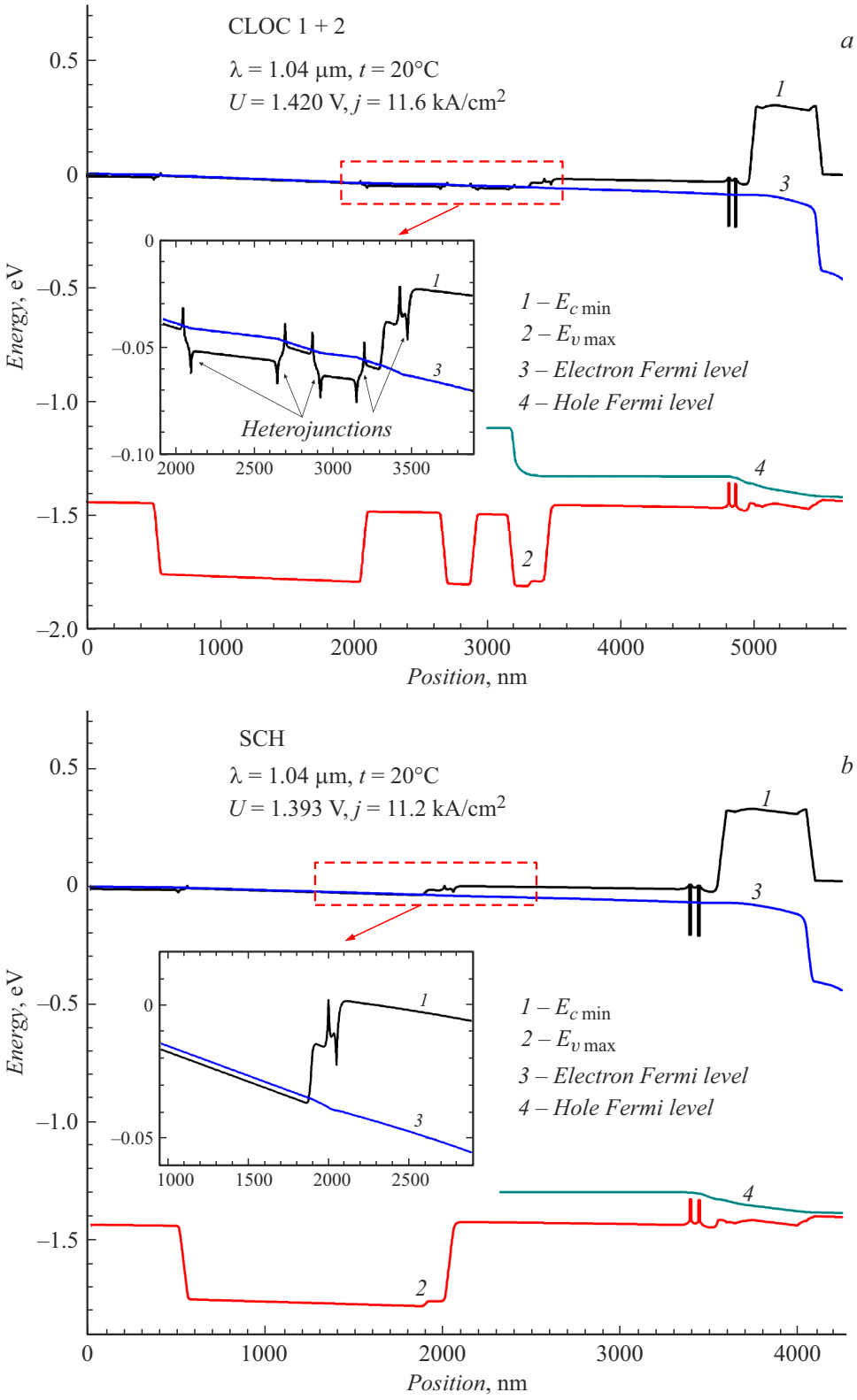

Figure 2. Energy band diagrams of CLOC 1+2 (*a*) and SCH (*b*) lasers at the direct bias of $p-n$-junction. E_c and E_v — the bottom energies of the conduction band and valence band, respectively. The insets show the conduction band bottom energy and the quasi-Fermi level for electrons for the regions highlighted by the dashed lines on an enlarged scale.

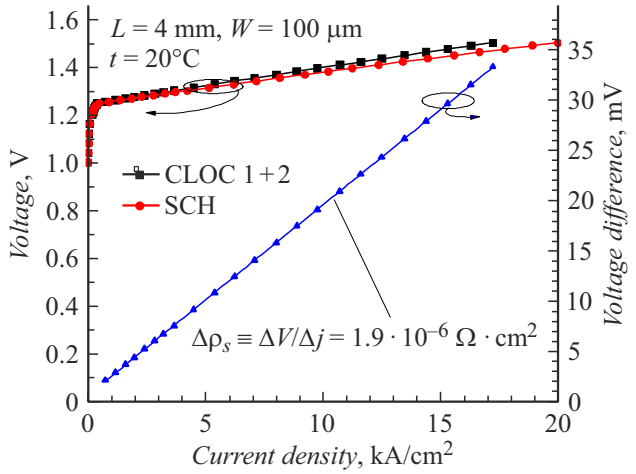

Figure 3. Simulated CV characteristics of the CLOC 1+2 and SCH lasers, and the dependence of the excess voltage in the CLOC heterostructure versus current density. $\Delta\rho_s$ — series resistance contribution due to coupled waveguides in the laser heterostructure, ΔV — increment of voltage drop difference, Δj — increment of current density.

Experimentally obtained series resistance of high-power edge-emitting lasers in CW mode

Laser design	R_s, mΩ	L, mm	W, μm	ρ_s, Ω · cm^2	λ, μm
PLD [8]	13	4	100	$5.2 \cdot 10^{-5}$	0.98
LOC [9]	20	4	90	$7.2 \cdot 10^{-5}$	0.91
EDAS [9]	16	4	90	$5.8 \cdot 10^{-5}$	0.91
EDAS [1]	5	4	300	$6.0 \cdot 10^{-5}$	0.98
CLOC [4]	22	4	100	$8.8 \cdot 10^{-5}$	1.03

Note. PLD — pump laser diode, LOC — large optical cavity, EDAS — extremely double asymmetric structure, CLOC — coupled large optical cavity.

than the experimentally obtained values of series resistance of modern high-power lasers.

Acknowledgments

The authors are grateful to HSE University for providing licensed software.

Funding

The work of A.S. Payusov and G.O. Kornyshov was supported by the Russian Science Foundation (project No 22-22-00557).

Conflict of interest

The authors declare that they have no conflict of interest.

References

[1] L. Wang, H. Qu, A. Qi, X. Zhou, W. Zheng, Opt. Lett., **47** (13), 3231 (2022). DOI: 10.1364/OL.452048
[2] D. Ban, E.H. Sargent, St.J. Dixon-Warren, K. Hinzer, J.K. White, A.J. SpringThorpe, IEEE J. Quantum Electron., **40** (6), 651 (2004). DOI: 10.1109/JQE.2004.828262
[3] N.Yu. Gordeev, A.S. Payusov, Y.M. Shernyakov, S.A. Mintairov, N.A. Kalyuzhnyy, M.M. Kulagina, M.V. Maximov, Opt. Lett., **40** (9), 2150 (2015). DOI: 10.1364/OL.40.002150
[4] A.E. Zhukov, N.Yu. Gordeev, Yu.M. Shernyakov, A.S. Payusov, A.A. Serin, M.M. Kulagina, S.A. Mintairov, N.A. Kalyuzhnyi, M.V. Maksimov, Tech. Phys. Lett., **44** (8), 675 (2018). DOI: 10.1134/S1063785018080151.
[5] A. Serin, N. Gordeev, A. Payusov, Y. Shernyakov, Y. Kalyuzhnyy, S. Mintairov, M. Maximov, J. Phys.: Conf. Ser., **929** (1), 012077 (2017). DOI: 10.1088/1742-6596/929/1/012077
[6] *STR soft* [Electronic source]. https://str-soft.com/devices/silense/
[7] N.A. Pikhtin, S.O. Slipchenko, Z.N. Sokolova, I.S. Tarasov, Semiconductors, **38** (3), 360 (2004). DOI: 10.1134/1.1682615.
[8] V. Gapontsev, N. Moshegov, I. Berezin, A. Komissarov, P. Trubenko, D. Miftakhutdinov, I. Berishev, V. Chuyanov, O. Raisky, A. Ovtchinnikov, Proc. SPIE, **10086**, 1008604 (2017). DOI: 10.1117/12.2250634
[9] K.H. Hasler, H. Wenzel, P. Crump, S. Knigge, A. Maasdorf, R. Platz, R. Staske, G. Erbert, Semicond. Sci. Technol., **29** (4), 045010 (2014). DOI: 10.1088/0268-1242/29/4/045010

Translated by Ego Translating